3706 *Inorg. Chem.* **2010**, *49*, 3706–3713
DOI: 10.1021/ic901387q

Inorganic Chemistry
Article

Electroabsorption of Dimers Containing MM (M = Mo, W) Quadruply Bonded Units: Insights into the Electronic Structure of Neutral Coupled Redox Centers and Their Relationship with Mixed Valence Ions

Malcolm H. Chisholm,*,† Benjamin J. Lear,† Alberto Moscatelli,‡ and Linda A. Peteanu*,‡

†*Department of Chemistry, The Ohio State University, Columbus, Ohio 43210, and* ‡*Department of Chemistry, Carnegie Mellon University, Pittsburgh, Pennsylvania 15213*

Received July 15, 2009

The electroabsorption spectra for the metal-to-ligand charge transfer transition in complexes containing oxalate and terephthalate bridged MM quadruply bonded units, $[(MM)(pivalate)_3]_2$-μ_2-BR, where M = Mo or W and BR = oxalate or terephthalate, are reported. The measured magnitude of the change in dipole moment ($|\Delta\vec{\mu}|$) and the change in polarizability ($\Delta\alpha$) that accompany this electronic transition are found to be small and not to follow the behavior expected on the basis of the two-state model. In addition, the trend in the value of $\Delta\alpha$ for the neutral states is mirrored by the trend in the degree of electronic coupling ($\mathbf{H_{AB}}$) for the strongly coupled mixed valence states formed by the same complexes in their singly oxidized states.

Introduction

Electroabsorption (EA) spectroscopy (also known as Stark spectroscopy) is a powerful means of characterizing electronic transitions. By the application of an external electric field, it permits the measurement of the magnitude of the change in dipole moment, $|\Delta\vec{\mu}|$, and the trace of the change in polarizability, $\mathrm{Tr}(\Delta\alpha)$, associated with an electronic transition.

The ability to determine $|\Delta\vec{\mu}|$ has been exploited heavily in the study of inorganic and bioinorganic complexes in which the magnitude and direction of $|\Delta\vec{\mu}|$ contains a great deal of information concerning the nature of the electronic transition.[1−14] Use of EA spectroscopy on intervalence charge transfer (IVCT) bands has allowed for the classification of mixed valence species within the Robin−Day classification scheme.[15] Specifically, those complexes with large $|\Delta\vec{\mu}|$ values are assumed to possess an electronically localized ground state (Class II), while an electronically delocalized ground state (Class III) is assigned to those complexes with a small or zero $|\Delta\vec{\mu}|$ value. The utility of EA for assignment of complexes as localized or delocalized has applications for the study of the localized-to-delocalized transition in mixed valence complexes, a topic of considerable recent interest.[16−18]

Despite the fact that, under several models of mixed valence chemistry,[19−21] the metal-to-ligand charge transfer (MLCT) or the ligand-to-metal charge transfer bands should contain as much information as the IVCT bands concerning the extent of electronic coupling, the former have received

*To whom correspondence should be addressed. E-mail: chisholm@chemistry.ohio-state.edu (M.H.C.), peteanu@andrew.cmu.edu (L.A.P.).

(1) Silverman, L. N.; Kanchanawong, P.; Treynor, T. P.; Boxer, S. G. *Phil. Trans. Roy. Soc. A* **2008**, *366*, 33–45.
(2) Oh, D. H.; Sano, M.; Boxer, S. G. *J. Am. Chem. Soc.* **1991**, *113*, 6880–6890.
(3) Bublitz, G. U.; Boxer, S. G. *Annu. Rev. Phys. Chem.* **1997**, *48*, 213–242.
(4) Chowdhury, A.; Peteanu, L. A.; Webb, M. A.; Loppnow, G. R. *J. Phys. Chem. B* **2001**, *105*, 527–534.
(5) Boxer, S. G. *J. Phys. Chem. B* **2009**, *113*, 2972–2983.
(6) Shin, Y. K.; Brunschwig, B. S.; Creutz, C.; Sutin, N. *J. Phys. Chem.* **1996**, *100*, 8157–8169.
(7) Dinolfo, P. H.; Hupp, J. T. *J. Am. Chem. Soc.* **2004**, *126*, 16814–16819.
(8) Karki, L.; Vance, F. W.; Hupp, J. T.; LeCours, S. M.; Therien, M. J. *J. Am. Chem. Soc.* **1998**, *120*, 2606–2611.
(9) Lockhart, D. J.; Boxer, S. G. *Proc. Natl. Acad. Sci. U.S.A.* **1988**, *85*, 107–111.
(10) Schatz, P. N.; Piepho, S. B.; Krausz, E. R. *Chem. Phys. Lett.* **1978**, *55*, 539–542.
(11) Shin, Y. K.; Brunschwig, B. S.; Creutz, C.; Sutin, N. *J. Am. Chem. Soc.* **1995**, *117*, 8668–8669.
(12) Steffen, M. A.; Lao, K.; Boxer, S. G. *Science* **1994**, *264*, 810–816.
(13) Walters, K. A.; Kim, Y.; Hupp, J. T. *Inorg. Chem.* **2002**, *41*, 2909–2919.
(14) Walters, K. A.; Premvardhan, L. L.; Liu, Y.; Peteanu, L. A.; Schanze, K. S. *Chem. Phys. Lett.* **2001**, *339*, 255–262.
(15) Robin, M. B.; Day, P. *Adv. Inorg. Chem. Radiochem.* **1967**, *10*, 247–422.
(16) Concepcion, J. J.; Dattelbaum, D. M.; Meyer, T. J.; Rocha, R. C. *Phil. Trans. R. Soc. A* **2008**, *366*, 163–75.
(17) Demadis, K. D.; Hartshorn, C. M.; Meyer, T. J. *Chem. Rev.* **2001**, *101*, 2655–2685.
(18) Lear, B. J.; Glover, S. G.; Londergan, C. H.; Salsman, J. C.; Kubiak, C. P. *J. Am. Chem. Soc.* **2007**, *129*, 12772–12779.
(19) Brunschwig, B. S.; Creutz, C.; Sutin, N. *Chem. Soc. Rev.* **2002**, *31*, 168–184.
(20) Ondrechen, M. J.; Ko, J.; Zhang, L. T. *J. Am. Chem. Soc.* **1987**, *109*, 1672–1676.
(21) Nelsen, S. F.; Weaver, M. N.; Luo, Y.; Lockard, J. V.; Zink, J. I. *Chem. Phys.* **2006**, *324*, 195–201.

Published on Web 03/16/2010

Scheme 1. Complexes **1**−**5**

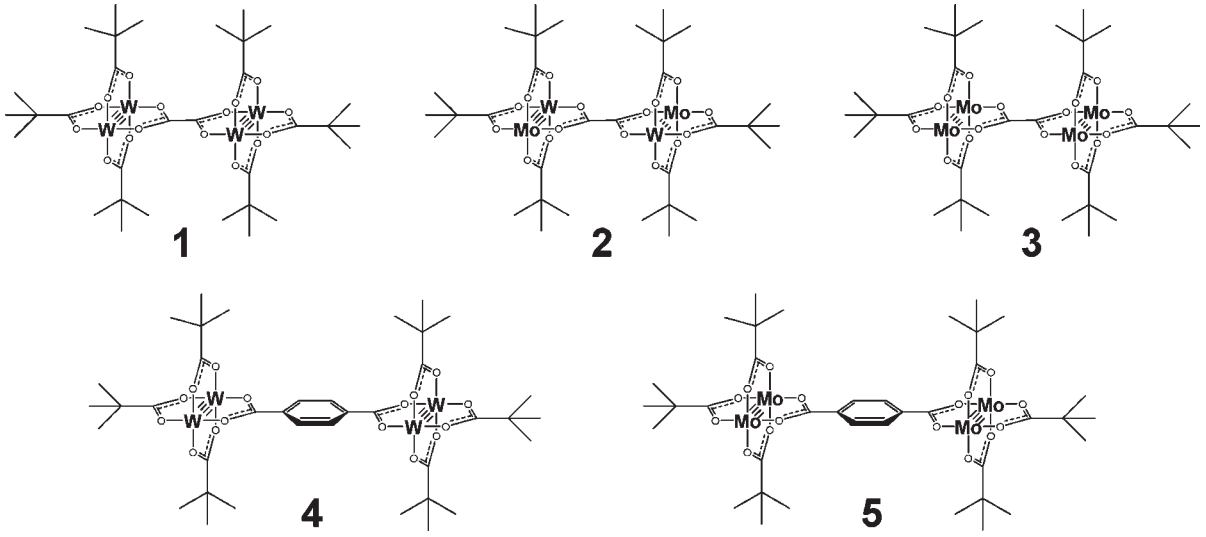

very little attention in the mixed valence literature. Previous reports of the EA of mixed valence complexes have focused on the mixed valence states[1,2,22] and few have addressed the MLCT transition.[2] Unlike the IVCT transition, the MLCT transition is present in both the neutral and the mixed valence states. As such, studies into the MLCT transition affords the opportunity to discuss relationships between properties, such as the degree of electronic coupling and delocalization, present in the neutral and mixed valence states. In addition, the MLCT transition has the ability to probe the interaction between metal and bridge in mixed valence complexes, which is seen as critical in determining the magnitude of electronic coupling. For this reason, we report on five neutral (non-mixed valence) MM quadruply bonded complexes of the type $[(MM)(pivalate)_3]_2$-μ_2-BR, where M = Mo or W and BR = oxalate or terephthalate (Scheme 1). These complexes form strongly coupled mixed valence species in their +1 oxidation state,[23] and we expect that the information gained from the EA of the neutral species will complement our understanding of the mixed valence state. In addition, the MLCT excited states of the neutral states of mixed valence ions will be interesting in their own right as they possess the correct connectivity either to form excitons, in which the hole is delocalized over the two MM units, or to exhibit excited state mixed valency.[24]

Experimental Section

Chemicals. Compounds **1**−**5** were prepared using published procedures.[25] Solvents were obtained from Fisher Scientific and dried using standard techniques. All manipulations were carried out under a purified N_2 atmosphere by using standard procedures for the manipulation of air-sensitive materials.

Acquiring EA spectra. Samples were dissolved in 2-methyl tetrahydrofuran (2-Me THF) and placed in an optical cell inside the glovebox. The optical cell consisted of two glass slides coated with indium tin oxide (surface resistivity 70−100 $\Omega \cdot sq^{-1}$, Aldrich) and a 220 μm thick Kapton tape spacer sandwiched between them. At the center of the spacer an approximately 5 by 10 mm window was cut out to accommodate the sample. The optical cell was held together by two binder clips. Immediately after removal from the glovebox, the sample was immersed into an optical Dewar filled with liquid nitrogen.

EA spectra were obtained using a homemade Stark spectrometer consisting of a 150 W xenon lamp (Osram) whose output was focused onto the entrance slit of a 0.15 m monochromator (Acton). Monochromatic light was first depolarized and then horizontally repolarized before being focused to the sample. Transmitted light was collected into a photodiode (UDT Sensors) operating in photovoltaic mode. The signal was preamplified before reaching a lock-in amplifier (Stanford Instruments) locked at the frequency of the applied electric field (465 Hz, Joseph Rolfe high-voltage power supply), and set to acquire at the second harmonic of the signal. The sample cell was oriented such that the applied electric field and the polarization of the incident light were at the magic angle (χ = 55°). The field strength used was 0.18 $MV \cdot cm^{-1}$.

Fitting the EA Spectrum. To minimize instrumental artifacts on the values of $|\Delta\vec{\mu}|$ and $Tr(\Delta\alpha)$, the absorption spectrum at liquid nitrogen temperature used for fitting was acquired in the same spectrometer used for EA measurements. An optical chopper modulated the signal for the lock-in amplifier (frequency 175 Hz), the latter set to acquire at the first harmonic of the signal. Absorption spectra were obtained from the transmission spectra of the sample and the solvent alone. Samples were prepared so that the maximum absorbance value for the MLCT band fell between 0.8 and 1.4.

The Stark effect and the fitting of EA spectra have been addressed in detail elsewhere[3,4] and are based upon Liptay's treatment for an isotropically oriented sample.[26] We followed similar procedures for the analysis of the spectra reported herein. The change in the absorbance, $\Delta A(\tilde{\nu})$, upon applying an external electric field ($\vec{F}$) is the linear combination of the zeroth, first, and second derivative of the field-off absorption spectrum, $A(\tilde{\nu})$:

$$\Delta A(\tilde{\nu}) = f^2\vec{F}^2\left[A_\chi A(\tilde{\nu}) + B_\chi \frac{\tilde{\nu}}{15\hbar}\frac{\partial}{\partial\tilde{\nu}}\left(\frac{A(\tilde{\nu})}{\tilde{\nu}}\right) + C_\chi \frac{\tilde{\nu}}{30\hbar}\frac{\partial^2}{\partial\tilde{\nu}^2}\left(\frac{A(\tilde{\nu})}{\tilde{\nu}}\right)\right] \quad (1)$$

The coefficients A_χ, B_χ, and C_χ were determined using the least-squares algorithm. At the magic angle, employed for

(22) Oh, D. H.; Boxer, S. G. *J. Am. Chem. Soc.* **1990**, *112*, 8161–8162.
(23) Chisholm, M. H.; Patmore, N. J. *Acc. Chem. Res.* **2007**, *40*, 19–27.
(24) Lockard, J. V.; Zink, J. I.; Konradsson, A. E.; Weaver, M. N.; Nelsen, S. F. *J. Am. Chem. Soc.* **2003**, *125*, 13471–13480.
(25) Cayton, R. H.; Chisholm, M. H.; Huffman, J. C.; Lobkovsky, E. B. *J. Am. Chem. Soc.* **1991**, *113*, 8709–24.
(26) Liptay, W. In *Excited States*; Academic Press: New York, 1974; Vol. *1*, pp 129−229.

these measurements, the equations for A_χ, B_χ, and C_χ become, respectively,

$$A_{55^\circ} = \frac{1}{3|\vec{m}|^2}\sum_{i,j}\mathbf{A}^2 + \frac{2}{3|\vec{m}|^2}\sum_{i,j}\vec{m}_i\mathbf{B} \quad (2)$$

$$B_{55^\circ} = \frac{10}{|\vec{m}|^2}\sum_{i,j}\vec{m}_i\mathbf{A}\Delta\vec{\mu}_j + \frac{15}{2}\langle\Delta\alpha\rangle \quad (3)$$

and

$$C_{55^\circ} = 5|\Delta\vec{\mu}|^2 \quad (4)$$

where m_i is the transition moment, **A** is the transition polarizability, and **B** is the transition hyperpolarizability. **A** and **B** describe the effect of an electric field on the transition moment: $\vec{m}(\vec{F}) = \vec{m} + \mathbf{A}\cdot\vec{F} + \vec{F}\cdot\mathbf{B}\cdot\vec{F}$. Though two terms contribute to B_{55° we neglect the first term to extract $\langle\Delta\alpha\rangle$ directly from this fitting coefficient. We justify the neglect of the first term based on several lines of reasoning. First, it has been argued that the transition moment hyperpolarizability will be large only if the transition moment itself is very large.[27] This is not the case for the complexes studied here as their extinction coefficients are all less than 40,000 M^{-1} cm^{-1}. Second, the contribution of the zeroth derivative to the fitting of the spectra shown here is negligible. This would imply that both terms in the expression for A_{55° in eq 2 are small. Though it is possible that these two terms can be large but of opposite sign and therefore cancel, this appears unlikely as B is the second term in the perturbation expansion while A is the leading term and the transition moments themselves are between 4 and 11 D. Finally, the change in dipole moment extracted from C_{55° is small for all of the compounds studied here (see below), also suggesting that the first term in eq 2 can be neglected. If this is the case, then B_{55° is given as

$$B_{55^\circ} = \frac{15}{6}\mathrm{Tr}(\Delta\alpha) \quad (5)$$

where $\mathrm{Tr}(\Delta\alpha) = 3\langle\Delta\alpha\rangle$, allowing $\mathrm{Tr}(\Delta\alpha)$ to be obtained from the first derivative of the EA spectrum (eq 1). The value of $|\Delta\vec{\mu}|$ is extracted directly from the second derivative coefficient C_{55° (eq 4).

The values of $|\Delta\vec{\mu}|$ and $\mathrm{Tr}(\Delta\alpha)$ are necessarily scaled by f and f^2 respectively, where f is the local field factor and is usually taken to be between 1.1 and 1.3 in organic solvents. This scaling takes into account the fact that the electric field experienced by the molecules in the sample is not the same as the applied external field.[5] As in the current study we are less concerned with absolute values of $|\Delta\vec{\mu}|$ and $\mathrm{Tr}(\Delta\alpha)$ and more with the *trends* in these values, our interpretation does not rely on the accurate determination of f.

The uncertainty values for $|\Delta\vec{\mu}|$ and $\mathrm{Tr}(\Delta\alpha)$ in Table 1 were estimated by multiple measurements at different dilutions and at different field strengths. For all complexes, one set of parameters fits the whole spectrum within the error limits reported, except for compound **1**, for which simulations that included the lowest energy vibronic band resulted in output values inconsistent with respect to the rest of the EA spectrum (see Supporting Information).

Stark Effect. Here we provide a simple picture for interpreting the Stark effect in **1**−**5** (Figure 1). We note that this picture is regarded as the "classical" Stark effect and that more complex behavior, notably dependence of the derived parameters on vibronic level, have been treated in the literature as well.[28−30] The sample is frozen in the absence of an electric field resulting in a random distribution and orientation of the molecules and their dipole moments. Once the sample is frozen, application of the electric field is assumed not to change the orientation of the molecules. It does, however, affect the energies of electronic transitions in predictable ways.

As seen in Figure 1a, if the electronic transition is accompanied by a change in dipole moment, $|\Delta\vec{\mu}|$, then the application of an electric field causes the energy of this transition to be dependent upon the orientation of the molecules. The electronic transition for those molecules that are oriented such that the change in their dipole moment is parallel to the electric field will be reduced in energy and those for which the change in dipole moment is antiparallel will be raised in energy relative to the transition at zero field. This arises from simple electrostatic considerations. As a result, the band structure for the electronic transition will be broadened by the application of the electric field (Figure 1b). Since EA spectra are reported as the difference between the spectra with and without the application of an electric field, the contribution arising from the change in dipole moment results in an EA spectrum that has the shape of the second derivative of the zero field absorption band (Figure 1c). The contribution from $\Delta\alpha$ can be seen schematically in Figure 1d. Here, application of a field causes the dipole moment of the molecules to be biased in the direction of the field *regardless of molecular orientation*. If the polarizability is greater in the excited state than in the ground state, this necessarily results in a lowering of the transition energy for all molecules in the sample. Likewise, if the polarizability is higher in the ground state, this results in an increase in the transition energy. Both of these effects are observed as a shift in the position of the absorption band (Figure 1e for a positive $\Delta\alpha$) upon application of the field. Thus, the resulting EA spectrum will have the shape of the first derivative of the zero field absorption spectrum (Figure 1f). By analysis of the EA spectrum, we can gain insight into $|\Delta\vec{\mu}|$ and $\Delta\alpha$ for a particular electronic transition. In this study we report the difference in the trace of the polarizability tensors, $\mathrm{Tr}(\Delta\alpha)$. The value of the transition dipole moment for the transition between any two states i and j (μ_{ij}) can also be affected by application of an external electric field. This results in a contribution to the EA spectrum from the zeroth derivative of the absorption band. These parameters ($|\Delta\vec{\mu}|$, $\Delta\alpha$, $\Delta\vec{\mu}_{ij}$) are extracted by fitting the experimentally observed EA spectrum (Table 1).

Table 1. Values for the Observed Change in Dipole Moment $|\Delta\mu_{ag}|$, $\mathrm{Tr}(\Delta\alpha)$, and $\mathbf{H_{AB}}$ for **1**−**5** Obtained from Simulation of the Electroabsorption Spectra (Figure 2); Also Given Are the Calculated Transition Dipole Moment $|\mu_{ga}|$ and the Diabatic Change in Dipole Moment $\Delta\mu_{12}$

compound	$\lvert\Delta\mu_{ag}\rvert$ (D)	$\mathrm{Tr}(\Delta\alpha)$ ($Å^3$)	$\mathbf{H_{AB}}^a$ (cm^{-1})	$\lvert\mu_{ga}\rvert$ (D)	$\Delta\mu_{12}$ (D)
1	0.5 ± 0.3	14 ± 5	2980	8.3	16.5
2	0.5 ± 0.2	52 ± 4	2540	7.3	14.6
3	0.8 ± 0.1	140 ± 20	2000	6.4	12.4
4	1.0 ± 0.2	200 ± 40	1610	11.7	23.4
5	3.0 ± 0.1	410 ± 10	∼400	4.7	9.78

[a] Estimates of $\mathbf{H_{AB}}$ come from refs 23 and 31.

Results and Discussion

The EA spectrum and associated fit for complexes **1**−**5** are shown in Figure 2, and the parameters derived are summarized in Table 1. With the exception of complex **1**,

(27) Parson, W. W. *Modern Optical Spectroscopy with Examples from Biophysics and Biochemistry*; Springer Verlag: Berlin, Germany, 2007.

(28) Reimers, J. R.; Hush, N. S. *J. Phys. Chem.* **1991**, *95*, 9773–9781.

(29) Reimers, J. R.; Hush, N. S. *NATO ASI series, Series C, Mathematical and Physical Sciences*; Proceedings of the NATO Advanced Workshop on Mixed Valency Compounds.; **1990**; Vol. *343*, pp 29−50.

(30) Treynor, T. P.; Boxer, S. G. *J. Phys. Chem. A* **2004**, *108*, 1764–1778.

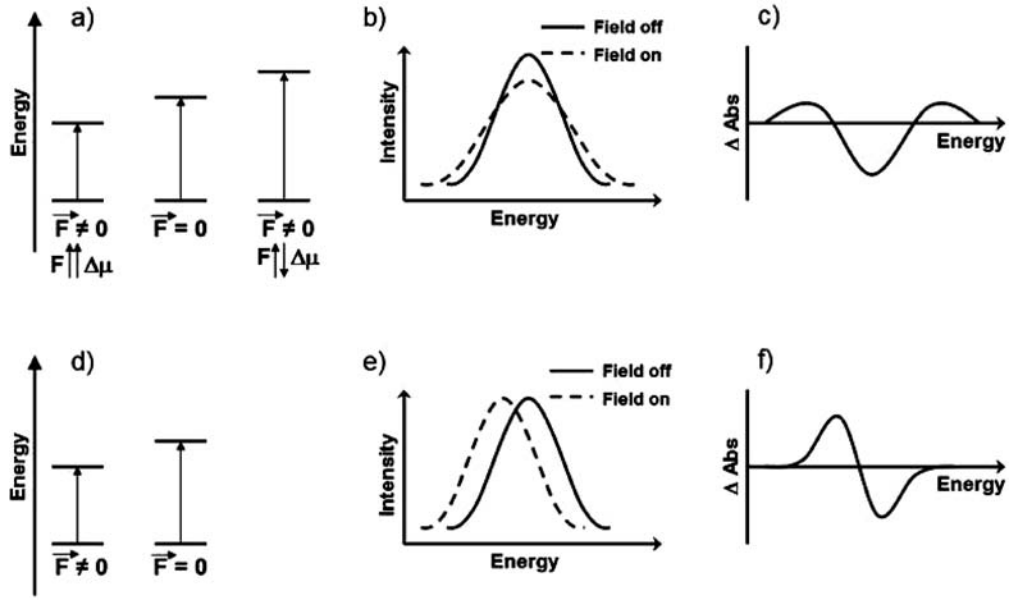

Figure 1. (a) Upon the application of an external electric field, the energy of an electronic transition is raised or lowered depending on whether the direction of $|\Delta\vec{\mu}|$ is in the same direction or opposed to the applied field. (b) This results in the broadening of the band associated with that transition. (c) This, in turn, means that the resulting EA spectrum will have the shape of the 2nd derivative of the absorption spectra for zero applied field. (d) Likewise, the change in polarizability ($\Delta\alpha$) can affect the energy of an electronic transition upon the application of an external electronic field. Depending on whether $\Delta\alpha$ is positive or negative, the energy of the transition will be reduced or increased; however, the change will be the same for *all molecules* in the sample. (e) This results in a shift in the energy (shown here for a positive value of $\Delta\alpha$) of the band and gives rise to an EA spectrum (f) that resembles the 1st derivative of the absorption spectrum taken in the absence of an applied field.

generally high quality fits are obtained of the main MLCT transition using a single set of parameters despite the possibility of overlap with nearby transitions having different electronic character. Specifically, some of the deviation observed between the EA spectra and the fit on the higher energy side may be due to overlap with a strong $\pi-\pi^*$ transition nearby.[25,31] Therefore, with the possible exception of complex **1**, the variation in electronic properties with vibronic level, predicted[28−30] and measured for the *intervalence* charge transfer bands of several other complexes,[2,22] is not obvious here.

In the case of complex **1**, simultaneous fitting of the entire MLCT band gives a poor quality fit (see Supporting Information) which is significantly improved if, as is shown in Figure 2, the lowest energy band (~13000 cm^{-1}) is excluded from the fit. One possible reason for this is the presence of a weak low energy transition in the spectrum of this compound that remains unidentified but which may be a ^{3}MLCT ← $^1S_0$ transition. Interestingly, the parameters obtained from the fit shown in Figure 2 (the fit of the full MLCT band) and a fit in which the lowest energy transition and the remainder of the spectrum fit independently are surprisingly similar (see Supporting Information). This highlights the sensitivity of the Stark spectrum to very modest differences in electronic properties across a spectral band. Another possible interpretation of this finding is that **1** exhibits more strongly non-Condon behavior than do the other complexes, meaning that the degree of charge transfer in this complex depends on the displacement along particular vibrational coordinates.[2,28−30,32] The band which cannot be fitted using the analysis used here appears to be the origin of a vibronic progression of frequency ~1500 cm^{-1} that is evident in the absorption spectrum of **1** (Figure 2) and which has been assigned as symmetric stretch of the bridging ligand. This has been treated in more detail elsewhere.[33,34] While we cannot, at this point, discriminate between these two possibilities, we again note that the response of the first vibronic feature of this band to the field is not very different from that of the other members of the progression (Supporting Information).

Of note is that, for all five complexes, the EA spectrum is dominated by the first derivative of the corresponding absorption spectrum. The relative contribution of the second derivative is small but increases across the series **1**−**5**. For all spectra, the zeroth derivative contribution is also small, suggesting that the value of the transition dipole moment is not significantly affected by the application of the external field. This, in turn, allows us to obtain values of $|\Delta\vec{\mu}|$ and Tr($\Delta\alpha$) for **1**−**5** from the fitting of the associated EA spectra (vide supra). The trends in the values of $|\Delta\vec{\mu}|$ and Tr($\Delta\alpha$) across the series of **1**−**5** are examined in detail below.

Concerning $|\Delta\vec{\mu}|$. For all five complexes, $|\Delta\vec{\mu}|$ is much smaller than would be expected from the transfer of a unit of charge from a state entirely localized on one of the metal centers to a state entirely localized on the bridge. The crystallographic distances from the centroid of a MM unit to the centroid of the bridge is 3.48 Å for **1**−**3** and 5.65 Å for **4** and **5**.[35,33] These give a calculated "crystallographic" change in dipole of 17 D for **1**−**3** and 27 D for **4** and **5** which is much larger than the observed value. The overestimation of $|\Delta\vec{\mu}|$ by such simple methods is a well-known phenomenon in this field. Mitigation of $|\Delta\vec{\mu}|$ is

(31) Chisholm, M. H.; Feil, F.; Hadad, C. M.; Patmore, N. J. *J. Am. Chem. Soc.* **2005**, *127*, 18150–18158.
(32) Oh, D. H.; Boxer, S. G. *J. Am. Chem. Soc.* **1990**, *112*, 8161–8162.
(33) Bursten, B. E.; Chisholm, M. H.; Clark, R. J. H.; Firth, S.; Hadad, C. M.; MacIntosh, A. M.; Wilson, P. J.; Woodward, P. M.; Zaleski, J. M. *J. Am. Chem. Soc.* **2002**, *124*, 3050–3063.
(34) Lear, B. J.; Chisholm, M. H. *Inorg. Chem.*
(35) Cotton, F. A.; Donahue, J. P.; Lin, C.; Murillo, C. A. *Inorg. Chem.* **2001**, *40*, 1234–1244.

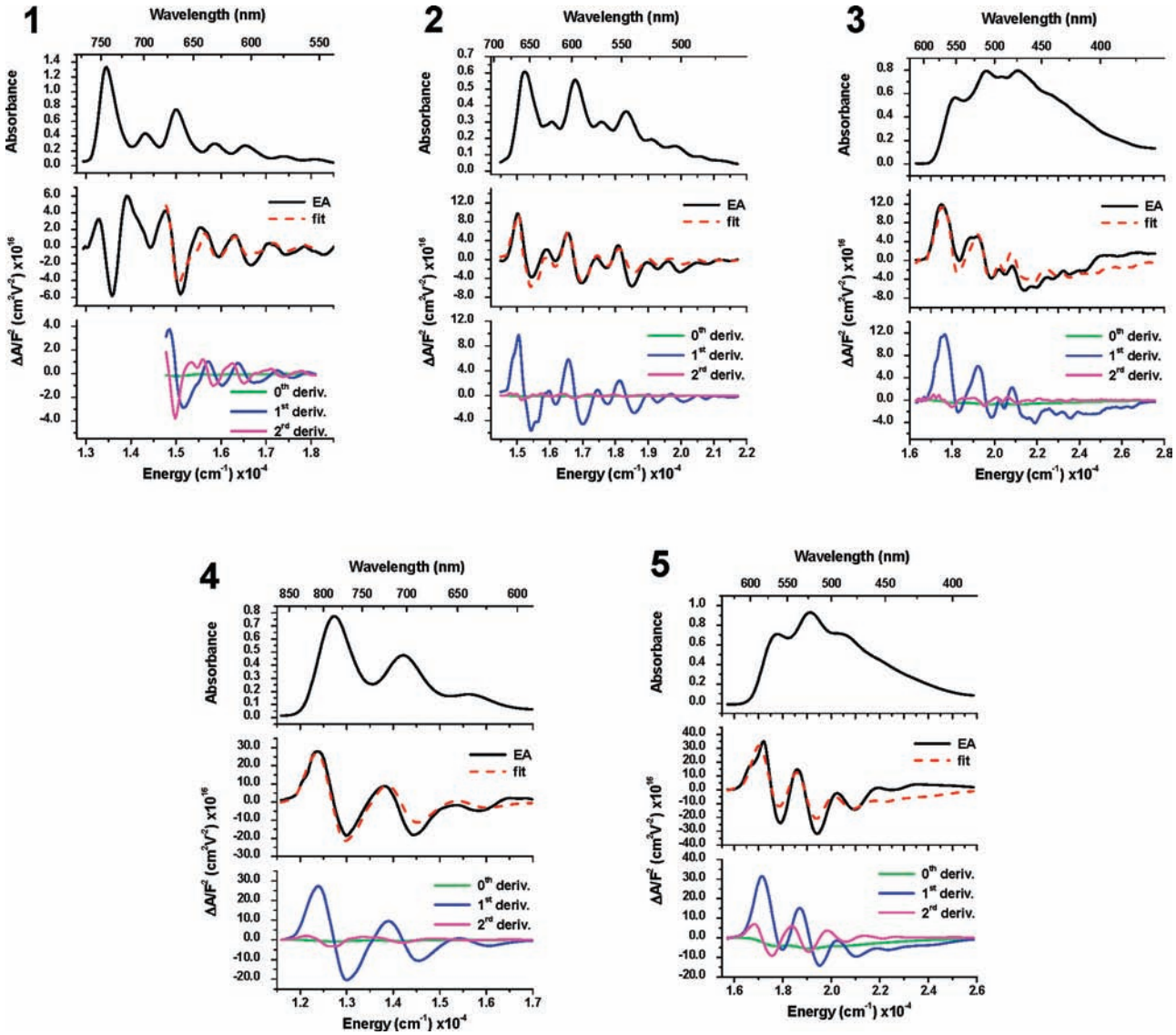

Figure 2. (Top) Absorption spectra at 77 K in 2-Me THF for **1**−**5**. (Middle) Experimental (black) and simulated (dashed red) electroabsorption spectra for **1**−**5**. (Bottom) Contributions to the fitting of the EA spectra from the 0th (green), 1st (blue), and 2nd (pink) derivative of the absorption spectra for **1**−**5**.

often ascribed to the effects of covalent bonding between chemical moieties and electronic coupling between the states involved in the electronic transition. To examine the latter we have also utilized the approach used by Shin et al. to calculate diabatic changes in dipole moments, and these are listed in Table 1 for **1**−**5**. It is clear that the calculated dipole moments are inconsistent with the observed $|\Delta\vec{\mu}|$ and indicate that the diabatic (or localized charge) model is not appropriate. However, this conclusion as well as the values of $|\Delta\vec{\mu}|$ we have determined by Stark spectroscopy is at odds with the experimentally observed solvatochromism[36] of these complexes at room temperature.[37] Thus, it remains to reconcile these two experimental observations.

These two apparently conflicting results can be understood by considering the Walsh diagram (Figure 3) for these complexes and by the fact that low temperature solvent dependence of **1**−**3** is much weaker than the room temperature solvent dependence.[38] Though the diagram in Figure 3 is strictly accurate only for **1**−**3**, similar behavior is expected for **4** and **5**. For **1**−**5**, it is the D_{2h} symmetry that is favored; however, the barrier to rotation through D_{2d} is quite small and a large range of geometries is expected at room temperature. Examination of Figure 3 shows that the expected dipole moment for the MLCT is dependent on the geometry. At D_{2h} geometry (enforced at the low temperatures employed for the Stark measurements), both the highest occupied molecular orbital (HOMO) and the lowest unoccupied molecular orbital (LUMO) are evenly distributed over the MM and bridge units, and the small $|\Delta\vec{\mu}|$ observed by Stark spectroscopy is expected for the MLCT transition. At room temperature, thermal energy will be sufficient for the average geometry of the molecules to be better described by D_2 symmetry. With an approach to the fully twisted geometry, D_{2d}, the

(36) Chowdhury, A.; Locknar, S. A.; Premvardhan, L. L.; Peteanu, L. A. *J. Phys. Chem. A* **1999**, *103*, 9614–9625.
(37) Chisholm, M. H.; Patmore, N. J. *Inorg. Chim. Acta* **2004**, *357*, 3877–3882.
(38) Lear, B. J.; Chisholm, M. H. *Inorg. Chem.* **2009**, *48*, 10954−10971.

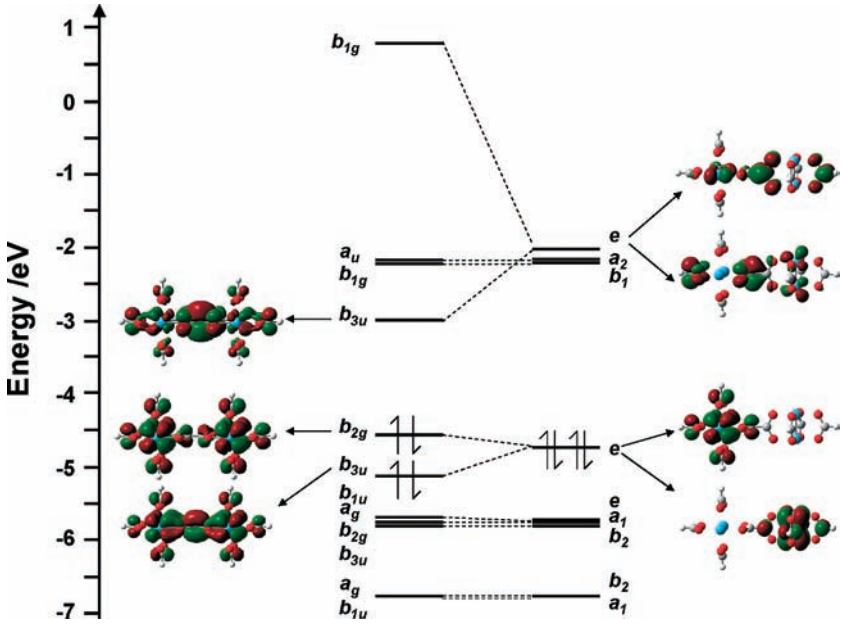

Figure 3. Walsh diagram for **1**−**3** showing the effect on the MM and bridge orbitals of moving between D_{2h} and D_{2d} geometry. Also shown are the orbitals involved in the MLCT transition, which occurs between the HOMO and LUMO under D_{2h} geometry and the HOMO and LUMO+2 under D_{2d} geometry. The orbitals shown are for **1** and have already been reported.

HOMO becomes increasingly localized on a single M_2 center. For this reason, the MLCT transition will result in a significant change in dipole moment for some of the molecules at room temperature, giving rise to the observed room temperature solvatochromism.

Across the series **1**−**5** there is no clear trend in $|\Delta\vec{\mu}|$. The values for **1**−**4** are each within (or very close to) the experimental error of one another. Interestingly, **1**−**4** are classified as Class III (or electronically delocalized) in their mixed valence oxidation state while **5** is assigned as Class II (or electronically localized) in its mixed valence oxidation state. Thus, perhaps the ground state mixed valence gives some indication of the extent of coupling in the excited state mixed valence state and vice versa (Figure 4). If this were the case, then it would make sense that Class III complexes display little change in dipole upon excitation of the MLCT and that Class II complexes would exhibit larger changes in dipole moment. It seems reasonable to expect the neutral states of strongly coupled mixed valence complexes to be themselves strongly coupled. However, it is equally clear that a delocalized electronic state for the mixed valence species does not necessitate a delocalized electronic state in the neutral species, and the current study is by no means exhaustive enough to make generalizations. However, this, as well as our recent studies, suggests[38] there is much to be learned from study of the MLCT transition in complexes that form mixed valence species.

Trend in Tr(Δα). Before we discuss the trend in Tr(Δα) it is useful to comment first on Δα itself, which is defined as the difference in polarizability of the ground state (α_g) and excited state (α_e) involved in the transition. Because we are interested in Tr(α), we can replace the transition moments with the scalar magnitude so that the polarizability of any state, *i*, is given[6] as

$$\mathrm{Tr}(\alpha) = 2\sum_{j\neq i}\frac{\mu_{ij}^2}{E_j - E_i} \qquad (6)$$

where μ_{ij} is the transition dipole moment between states *i* and *j*. Thus, we see that the polarizability for a particular state, α_i, is determined by both the transition dipole moment and the energy gap between that state and all the other electronic states of the molecule. Since it is difficult to know these values for the infinite number of electronic states, interpreting the magnitude of the change in polarizability using this equation is not simple.

To aid in the interpretation of Δα, one simplification that has been introduced is the two-state model.[28] In this model, the polarizabilities of the two electronic states involved in the transition of interest are taken to be completely determined by those same two states, rather than the infinite number of states that exist for the molecule. Therefore, for a transition between states (here involving the ground state), Δα is given by

$$\Delta\alpha = 2\left(\frac{\mu_{ge}^2}{E_g - E_e}\right) - 2\left(\frac{\mu_{eg}^2}{E_e - E_g}\right) = -4\left(\frac{\mu_{eg}^2}{E_e - E_g}\right) \qquad (7)$$

In this equation, E_e and E_g are the energies of the excited and ground state, respectively, and μ_{eg} is the transition dipole moment between these states. Though this certainly simplifies the calculation of Δα, the results that we find for **1**−**5** do not fit the predictions of the two-state model. Specifically, this model predicts that as $|\Delta\vec{\mu}|$ goes to zero, Δα will reach a maximum in the negative sense.[6] Instead, we find (Table 1) that both $|\Delta\vec{\mu}|$ and Tr(Δα) increase simultaneously and, more importantly, Tr(Δα) is *positive*. The simplest interpretation of this result is that in addition to the ground state, there are other electronic states that lie close in energy to and have significant transition dipole moments to the excited state.

The fact that Tr(Δα) is positive also indicates that these additional electronic states must lie above that of the MLCT transition. This may be seen by reconsidering eqs 6 and 7 from which it can be shown that a positive value

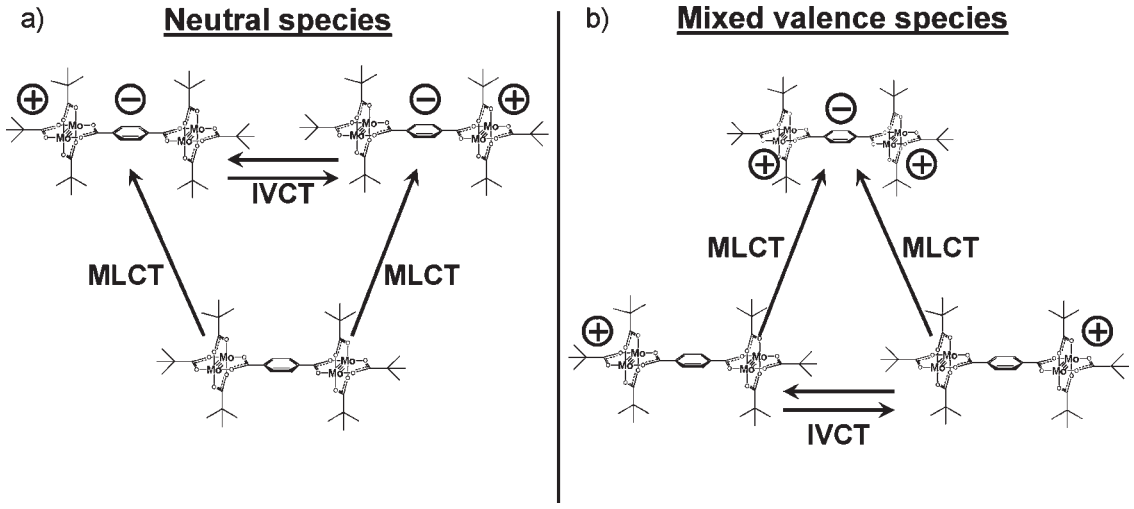

Figure 4. Comparison of the low energy charge transfer transitions possible in **1**−**5** for the neutral and mixed valence states using **5** as an example. Note that for both the neutral and the mixed valence species, MLCT and IVCT transitions are possible and that, in both cases, the MLCT transition involves degenerate states. For the neutral complexes, the degeneracy is in the excited state whereas for the mixed valence species, the degeneracy is in the ground state.

for $\Delta\alpha$ requires that the following expression to be true.

$$\sum_{i\neq e,g} \frac{(\mu_{ie})^2}{E_i - E_e} > 2\left(\frac{\mu_{eg}^2}{E_e - E_g}\right) + \sum_{i\neq e,g} \frac{(\mu_{ig})^2}{E_i - E_g} \qquad (8)$$

For this inequality to hold, a transition must exist from the excited state to a state that is higher in energy. In addition, for this higher energy state to increase the change in polarizability for the ^{1}MLCT transition, their energy separation should be small and/or the oscillator strength between them should be large. To begin, we envision three separate ways to describe the required electronic states. We can examine the Walsh diagram in Figure 3, where it can be seen that the LUMO+1 at D_{2h} geometry has opposite symmetry from that of the LUMO. Therefore, we might instead expect a strong transition from the ^{1}MLCT to a state involving electronic occupation of the LUMO+2. The fact that the energy gap of this transition is predicted to be smaller than that between the MLCT state and the ground state is also encouraging. Thus, the orbital structure returned by molecular calculations[33] suggest that there is a state above the ^{1}MLCT that is appropriate for explaining the trend reported here for Tr($\Delta\alpha$).

However, this is not the only state that we can imagine making a significant contribution to a positive Tr($\Delta\alpha$) for the MLCT transition. Excitation predominantly from one MM unit to the bridge (generating the ^{1}MLCT state) means that there are two degenerate ^{1}MLCT states (excitation from one MM unit or the other) as in Figure 4. This is a situation that is poised to couple these two MLCT excited states. We may think of this in terms of exciton theory, where such coupling can lead to "bright" and "dark" states[39] meaning the transition to them from the ground state has or does not have significant oscillator strength, respectively. These states are made up of combinations of the MLCT excitations. If the bright ^{1}MLCT state is lower in energy than the dark state, then, upon the MLCT transition, there will be a nearby higher energy state, which necessarily will have a significant transition dipole moment with the ^{1}MLCT state. This too could explain positive values of Tr($\Delta\alpha$).

There is yet a third way in which the required higher energy state could be envisioned. This is by invoking the concept of excited state mixed valency as introduced by Zink and co-workers.[24] Under this model, the degenerate MLCT states again may couple in the same way that degenerate redox states couple in ground state mixed valency. This must result in two states that, as the coupling increases, have an increasingly intense transition between them.[19] If the MLCT proceeds to the lower energy excited mixed valence state, this will leave a close-lying higher energy state with a significant transition dipole moment with the initially populated MLCT state, accounting for the positive value of Tr($\Delta\alpha$).

It is striking how similar the exciton and excited state mixed valence models are, and it is not clear what may distinguish one from the other. Perhaps in the future they will be shown to be identical treatments of the same phenomenon. All in all, we find that there are three possible explanations for a positive value of Tr($\Delta\alpha$). We are currently performing time-resolved transient absorption spectroscopy on these complexes, and the results of these experiments may illuminate the specific nature of the electronic states that lie above the MLCT excited state and provide further insight into the interplay between ground and excited state mixed valency.

In addition to the insight gained form eqs 6 and 7, $\Delta\alpha$ can be interpreted, using a crude physical picture, as being related to the spatial electronic distribution for a particular state.[2] Thus, to examine the trend in Tr($\Delta\alpha$) found in Table 1, we can consider the orbitals involved in the transition between the ground and MLCT states. For the diabatic (or localized) orbitals, the ground state will be entirely composed of the MM δ orbitals and the MLCT state will be entirely composed of the LUMO of the bridge. As the mixing between these orbitals increases, we expect that the percent composition of the MM δ orbitals and bridge LUMO will increase in the MLCT and ground states, respectively, reaching the limit (in *extremely* strong mixing) where both the ground and MLCT excited states are composed of equal parts of

(39) Scholes, G. D.; Rumbles, G. *Nat. Mater.* **2006**, *5*, 683–696.

MM δ and bridge LUMO orbitals. In this limit, and invoking this crude physical picture, the MLCT transition is not expected to result in a change in polarizability, yielding a value of Tr($\Delta\alpha$) of zero. In a case of weak (or zero) mixing, the value of Tr($\Delta\alpha$) will be determined by the diabatic orbitals referred to above, the sign of Tr($\Delta\alpha$) depending on whether the bridge LUMO is larger (positive Tr($\Delta\alpha$)) or smaller (negative Tr($\Delta\alpha$)) than the MM δ orbitals.

Using this approach, we suggest that in the case of **1**, the mixing of the orbitals is so strong that little change in polarizability is observed upon exciting the MLCT transition. A competing explanation would be that the MM δ orbitals and the bridge LUMO just happen to be of the same size for the oxalate bridged complexes. However, given that we observe a range of Tr($\Delta\alpha$) values for **1**−**3**, this does not seem likely. Tellingly, when the size of the bridge is increased, by moving from oxalate (**1**−**3**) to terephthalate (**4** and **5**) complexes, the values of Tr($\Delta\alpha$) also increase. The fact that Tr($\Delta\alpha$) is smaller for **4** than **5** (and for **1** than **3**) reflects the fact the WW δ orbital is higher in energy (better aligned with the bridge LUMO) than are the MoMo δ orbitals, resulting in greater mixing between the WW units and the bridge.

Lastly, we comment that we find a clear connection between values of Tr($\Delta\alpha$) in the non-mixed valence state and $\mathbf{H_{AB}}$ in the mixed valence state, namely, that as $\mathbf{H_{AB}}$ increases Tr($\Delta\alpha$) decreases. Creating similar electronic distributions between states is, of course, an expected function of $\mathbf{H_{AB}}$, as it directly mixes states and so the relationship between $\mathbf{H_{AB}}$ and Tr($\Delta\alpha$) can be explained via the physical picture just under discussion. However, increases in coupling should also result in increased transition intensity for the transitions described earlier (orbital, exciton, or mixed valence model). Thus, no matter the approach taken, we may explain the findings here that strong mixing of orbitals (and perhaps states) in non-mixed valence species seems to provide an indication of similar mixing in the mixed valence species. Whether or not this is a general result remains to be seen and will be the work of further study.

Conclusions

We have reported the electroabsorption spectra for the MLCT transition of a series of MM (M = W or Mo) quadruply bonded complexes. From these spectra, we find that the change in dipole moment ($|\Delta\vec{\mu}|$) is quite small, much smaller than would be expected from simple consideration of crystallographic data. Furthermore, Tr($\Delta\alpha$) increases with increasing length of the bridging ligand, as well as with increasing energy gap between the MM units and the bridge π^* orbitals. Despite the fact that these complexes are not in the mixed valence state, we find correlations between Tr($\Delta\alpha$) and the coupling in the mixed valence state ($\mathbf{H_{AB}}$), which leads us to speculate that there may be much to learn about the mixed valence state by examining the properties of the non-mixed valence states.

We also note that the trend in and sign of the values for Tr($\Delta\alpha$) do not agree with a simple two-state treatment of the transition and that additional states must be considered. We examined several ways in which the required states could be described. It seems likely that there is some excited state behavior, such as the formation of a delocalized exciton or excited state mixed valence system that gives rise to the trends that we observe. In the end, we conclude that the MLCT transition of strongly coupled mixed valence systems is of interest and that much can be learned about such complexes, even by examining the non-mixed valence redox-states. We hope to pursue this line of thought further in future studies.

Acknowledgment. M.H.C acknowledges NSF Grant CHE-0515835 and L.A.P. acknowledges NSF Grant CHE-079112 for financial support.

Supporting Information Available: Contains the results of various fitting strategies for complex **1**. This material is available free of charge via the Internet at http://pubs.acs.org.